Measurements and mechanisms of Thomson's jumping ring

Paul J. H. Tjossem and Victor Cornejo

Department of Physics, Grinnell College, Grinnell, Iowa 50112

Measurements of the phase delay of the current and force on a ring floated on a commonly available Thomson's jumping ring apparatus were performed for phase angles from 12° to 88°. The force and phase data show excellent agreement with a linear inductive model. We find that the demonstration, as usually performed with large highly conducting rings, operates in the inductance-dominated regime at 60-Hz line frequency. Stroboscopic photographs of the jumping ring, for both room-temperature and 78-K rings, confirm that the same time-averaged inductive phase lag mechanism, not an electrical transient, accounts for the jump height. We introduce a simple room-temperature demonstration that illustrates the importance of the phase lag: Despite its greater weight, a stack of thin rings will float higher than a single ring as the inductive phase lag comes to dominate the parallel resistance of the combined rings. © *2000 American Association of Physics Teachers.*

I. INTRODUCTION

Thomson's jumping ring[1] was first exhibited by Elihu Thomson[2] in 1887 and modified to include the ''floating ring'' variation by John A. Fleming in 1890.[3] This vivid demonstration of electromagnetic induction is still used in physics classrooms to illustrate Faraday's and Lenz's laws[4,5] and is the basis for linear actuators for servomechanical purposes[6] as well as induction heating[7] and rail guns.[8]

A conducting ring placed over the ferromagnetic core of a solenoid may levitate or jump off when the solenoid is supplied with sufficient 60-Hz alternating current. While the jumping ring effect is described in a number of textbooks[9,10] as simply the repulsion between a magnet (the solenoid) and an oppositely directed induced magnet (the ring), this explanation suffices only for a monotonic increase or decrease from zero current in the solenoid. Since, however, the demonstration is usually done with alternating current, the levitation requires either the inductive phase lag of the induced current in the ring to provide a time-averaged repulsive force,[1,5,11] or a sufficiently large electrical transient to induce a jump in the first quarter-cycle of the solenoid current.[12]

The importance of the inductive phase lag was recognized from the outset by Thomson[1,13] and has been discussed more recently in a number of theoretical treatments.[14–16] The experimental record, however, is less complete and more contradictory. Mak and Young,[17] in measurements on their own floating ring apparatus (which contained an unlaminated iron core), dismissed the inductive phase lag mechanism and proposed that phase delays in the magnetic core were dominant. Hall[18] used an apparatus identical to ours to explore the lifting force as a function of frequency over the range of 20–120 Hz, but did not examine the phases of the fields and current in the ring. Schneider and Ertel[12] have recently described a custom-built apparatus which operates in the inductive transient regime with a saturated iron core, using long tube-like rings.

In the present study, using a commonly available apparatus (CENCO Scientific),[19] we have measured the amplitudes and phases of the relevant quantities that cause the repulsive force on the floating ring, namely the radial component of the magnetic field due to the solenoid, B_ρ, and the current in the ring I_r (see Sec. III A). Over the frequency range of 20–900 Hz, the dominant mechanism requires the phase lag

of the current in the ring, and is in complete agreement with theoretical treatments by Page and Adams[14] and Saslow[15] (see Sec. II) in marked contrast to Mak and Young's[17] experimental results.

The explanation behind Thomson's jumping ring has been variously ascribed to time-averaged inductive phase lag,[14–16,18] core saturation effects,[12,17] and electromagnetic transients.[12] We took stroboscopic photographs (see Sec. III B), varied the initial phase of the applied voltage for both room temperature and 78-K rings, and performed numerical modeling to determine the relative importance of these effects for our standard apparatus.

II. THEORY

A sinusoidal current $I_s = I_{s0}\sin(\omega t)$ in the solenoid induces an emf $\mathcal{E}$ around the ring which drives current through the ring's impedance $\check{Z}$:

$$I_r = \frac{\mathcal{E}}{\check{Z}} = \frac{M\omega I_{s0}}{R_r^2 + \omega^2 L_r^2}[R_r\cos(\omega t) + \omega L_r\sin(\omega t)], \qquad (1)$$

where M is the mutual inductance between the ring and the solenoid, R_r is the ring's resistance, and L_r is the inductance of the ring in the presence of the solenoid and core.[14,15]

The field of the solenoid flares out at the top, giving rise to a radial component $B_\rho(z)$, such that[14,16]

$$B_\rho(z) = -\frac{\rho}{2}\frac{\partial B_z}{\partial z}. \qquad (2)$$

This B_ρ interacts with the ring current I_r to give a time-dependent upward force on the ring:

$$\vec{F} = \oint I_r d\vec{l} \times \vec{B}_\rho = 2\pi a I_r[B_\rho(z)]\hat{z}, \qquad (3)$$

where a is the radius of the ring. The vertical field at the center of the core is given approximately by $\vec{B}_z(0) = \mu n I_s\hat{z}$, with μ the effective permeability of the iron, which is assumed to behave linearly, without hysteresis or eddy currents and n is the number of wire turns per unit length. Since $B_\rho(z)$ is proportional to the solenoid current I_s, we may write

$$\vec{F} \propto \frac{2\pi a \mu M \omega I_{s0}^2}{R_r^2 + \omega^2 L_r^2} [R_r \cos(\omega t)\sin(\omega t) + \omega L_r \sin^2(\omega t)]\hat{z}. \quad (4)$$

The first term in the brackets arises from the part of the ring current which is in phase with the induced emf and is thus 90° out of phase with the solenoid current. It causes an oscillatory force at 2ω whose time average is zero. The second term, which comes from the inductive phase lag of the ring current, produces a time-averaged lifting force

$$\langle \vec{F} \rangle \propto \pi a \mu \frac{M}{L_r} I_{s0}^2 \frac{\omega^2 L_r^2}{R_r^2 + \omega^2 L_r^2} \hat{z} = \pi a \mu \frac{M}{L_r} I_{s0}^2 \sin^2 \delta \hat{z}, \quad (5)$$

where the magnitude of the phase angle δ of the induced current is given by

$$\sin \delta \equiv \frac{\omega L_r}{(R_r^2 + \omega^2 L_r^2)^{1/2}}. \quad (6)$$

For notational simplicity, the phase lag δ will be considered to be a positive quantity.

If the amplitude of the current I_{s0}, mutual inductance M, permeability μ, and height of the ring above the solenoid are held constant, Eqs. (5) and (6) predict that the vertical force on the ring is proportional to $\sin^2 \delta$, which may be written as

$$\langle F \rangle \propto \sin^2 \delta = \frac{1}{\left(\frac{R_r}{\omega L_r}\right)^2 + 1} = \frac{1}{\left(\frac{\omega_c}{\omega}\right)^2 + 1} = \frac{1}{\left(\frac{f_c}{f}\right)^2 + 1}, \quad (7)$$

where $\omega_c \equiv R_r / L_r$ is the so-called "corner frequency," the frequency at which the ring's resistance and inductive reactance $X_L = \omega L_r$ are equal. Equation (7) has the following limits:

$$\left(\omega \ll \frac{R_r}{L_r}\right) \quad \delta \approx \omega \frac{L_r}{R_r}, \quad \sin^2 \delta \approx \omega^2 \left(\frac{L_r}{R_r}\right)^2, \quad (8a)$$

$$\left(\omega = \omega_c = \frac{R_r}{L_r}\right) \quad \delta = 45°, \quad \sin^2 \delta = \frac{1}{2}, \quad (8b)$$

$$\left(\omega \gg \frac{R_r}{L_r}\right) \quad \delta \to 90°, \quad \sin^2 \delta \to 1. \quad (8c)$$

For frequencies much below the corner frequency, the force depends quadratically on ω and the ring's resistance. For frequencies considerably above the corner frequency, the force reaches a limit which is independent of both ω and the resistance of the ring.

III. EXPERIMENTAL ARRANGEMENT

The CENCO[19] solenoid consists of eight layers of 62 turns each of #14 (1.6-mm-diam) copper wire wound around a 4.45-cm outside diameter (o.d.) plastic form (see Fig. 1). The length of the solenoid is 12.5 cm, and it is fitted with 1.9 cm end caps which determine the closest approach of the ring. The magnetic core is a close-packed set of 30-cm-long #14 oxidized and annealed soft iron rods wrapped in a 3.49-cm-diam plastic sleeve. Over the full range of operating current, the core increases the inductance of the solenoid by a constant factor of 10, much less than the expected relative permeability ($\mu_r \gg 1000$) of the soft iron. This low enhancement is due mainly to the demagnetizing field set up by the magnetic poles, which reduces the relative permeability to about
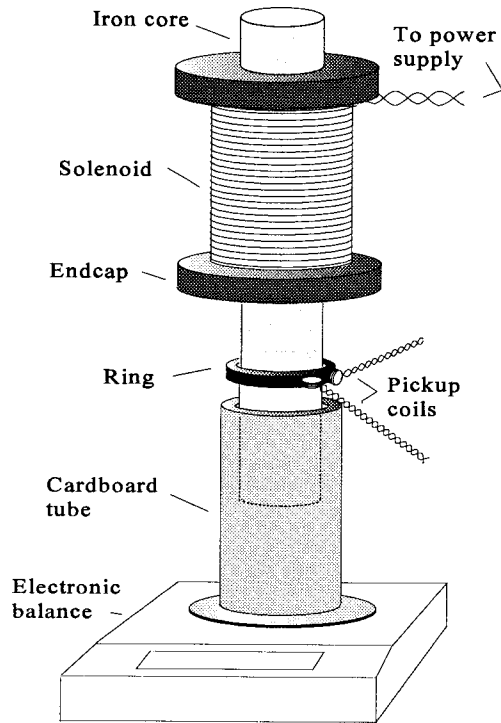

Fig. 1. The experimental apparatus consisting of the solenoid with laminated soft iron core is suspended from a wooden board (not shown) upside down over the electronic balance. A cardboard tube rests on the balance and holds the ring and a pair of small pickup coils. The time-averaged electromagnetic force on the ring is measured with the balance; the radial and vertical pickup coils measure the amplitudes and phases of the radial magnetic field and the current in the ring, respectively.

50 at the center of this short core, and considerably less toward the ends.[20] The inductance enhancement is further reduced because the core fills less than 40% of the average cross section of the solenoid windings.

The CENCO solenoid uses a cylindrical nickel-plated brass retaining clip (1.25 mm thick, 3.9 cm high) which wraps around the core and is slit vertically to clamp the iron core under pressure from a radial set screw.[21] Because this clip permits large eddy currents to flow opposite in direction to the ring current (which adds a short-range lifting force at high frequency) we removed it for these measurements. The apparatus is supplied with a large aluminum ring (6.0 cm o.d. × 4.0 mm thickness × 16.2 mm long), but for the present measurements we used a smaller, more resistive ring (5.1 cm o.d. × 3.18 mm thickness × 6.4 mm long) made from 6061-T6 aluminum alloy tubing. The increased resistance raised the corner frequency [Eq. (8b)] to a more convenient value for measuring the forces and phases.

A. Floating ring measurements

We measured the magnitude and phase of the emfs induced in a pair of small pickup coils (2.3 mm diameter) consisting of 10 turns each of #34 enameled copper wire placed just outside the radius of the ring (Fig. 1). The radially oriented coil measured the flux change due to B_ρ provided by the solenoid. The vertical pickup coil served as a side-look current transformer to measure the current in the ring, I_r. At the typical core extension of 10.2 cm, and in the absence of the ring, the solenoid produces negligible vertical magnetic field at the position of the pickup coils, which lie

outside of the core. Likewise, the ring produces negligible radial magnetic field for a radial pickup coil at the center of the plane containing the ring. Thus we measured the amplitudes and phases of I_r and B_ρ directly and independently, rather than inferring them from small differences between large axial flux measurements as was done in previous studies.[12,17] The vertical pickup coil was calibrated to measure the ring current by replacing the ring with a single loop of #12 copper wire and passing a known current through it.

A fast Fourier transform (FFT) network analyzer (Stanford Research Systems SR780) provided sine waves to a power booster (Kepco BOP-20-10M), which then drove a 115/24 VAC transformer wired backwards so as to step up the voltage to the solenoid. The current was set at 250 ± 0.5 mA rms, enough to give a measurable force without undue heating of the ring. The signals from the small pickup coils were sent to a high-impedance preamplifier (Princeton Applied Research 113) and then to the network analyzer. The phase of the solenoid current was monitored as a voltage drop across a small noninductive resistor in series with the solenoid.

The CENCO solenoid was removed from its steel base and attached upside down from a wooden frame. The ring and pickup coils were mounted on a cardboard tube which did not touch the iron core, but rested atop an electronic balance placed 35 cm below the inverted apparatus (see Fig. 1). The balance measured the reactive force needed to support the weight of the ring and cardboard tube. The repulsive (lifting, in the normal orientation) electromagnetic force on the ring increased the apparent weight of the ring on the balance.

For most of the measurements, the core was extended 10.2 cm above the surface of the solenoid and was held from above by the wooden support. In the absence of the ring, the pickup coils showed small phase shifts (0°–6° radial, 0°–9° vertical) from 10 to 900 Hz, due to hysteresis and eddy currents in the core.

B. Jumping ring measurements

The power required to make the ring jump exceeds our current-controlled capabilities. Instead, we operated the upright apparatus in the conventional voltage-controlled way: by connecting the solenoid to the 60-Hz power line through an autotransformer. We measured jump height for room temperature and liquid nitrogen-chilled rings, and took stroboscopic photographs during the jumps. A solid-state relay turned on the solenoid at a zero crossing of the power line voltage. A home-built circuit consisting of a zero-crossing detector, pulse synchronizer, and delay generator ensured that the stroboscopic images were synchronized with the start of the jump and at 1/60-s intervals thereafter. A binary counter limited the number of stroboscopic images to 8 or 16 in order to permit unambiguous identification on the photographic negative.

IV. RESULTS AND DISCUSSION

A. Phases

With the ring present, the phases of the ring current I_r and the radial field B_ρ are shown as a function of frequency in Fig. 2. The phases are measured relative to the trigger signal provided by the solenoid current. Since the pickup coils measure the time derivative of the magnetic flux, the raw signals from the coils have been integrated.
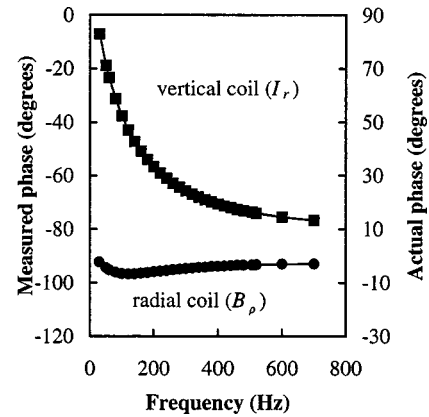

Fig. 2. The phases of B_ρ and I_r relative to the current in the solenoid as a function of frequency.

The phase shift of B_ρ with frequency remains approximately 0° from 30 to 700 Hz, despite the contribution the ring makes to the magnetization of the core.[17] While it differs from the shift observed without the ring, which went from 0° to +5° over this range, much of this difference can be attributed to slight contamination of the signal due to the vertical nonuniformity of the ring current. Since the primary magnetic field lines of the solenoid flare out [Eq. (2); also Ref. 4], the induced emf and current in the ring decrease with vertical distance from the center of the solenoid. This nonuniformity leads to incomplete cancellation of the radial component of the B field arising from the ring current and hence induces a small contaminating emf in the radial pickup coil.

The phase of the ring current begins at 90° at low frequencies (where the ring behaves like a pure resistance), passes through 45° at 120 Hz (this is the corner frequency $f_c = \omega_c/2\pi$ as given by Eq. (8b)), and then drops toward 0° in the inductance-dominated regime at high frequency. The phase lag δ of Eqs. (5)–(7) is thus the difference between the phase of I_r of Fig. 2 and 90°.

B. Force on the ring

The time-averaged lifting force $\langle F \rangle$ and $\sin^2 \delta$ for fixed solenoid current are plotted as a function of frequency in Fig. 3. The two curves follow each other closely, and in complete agreement with Eqs. (5)–(8) the force reaches half of its high-frequency limit at the 120-Hz corner frequency, when $\delta = 45°$. Thus the inductive phase lag mechanism accounts entirely for the force on the ring and we conclude that the eddy currents in the core of the apparatus are unimportant. This result contrasts with the findings of Mak and Young[17] whose solid iron core, more prone to eddy currents than our laminated core, could have obscured the mechanism explained above. Figure 4 shows the time-averaged force $\langle F \rangle$ vs $\sin^2 \delta$, in complete agreement with Eq. (5).

The Lorentz force [Eq. (3)] can be calculated directly from the measured amplitudes of the radial magnetic field and the ring current, the ring diameter, and the phase factor [Eq. (7)]. With 0.250 A rms in the solenoid at 120 Hz, $B_\rho = (1.30 \times 10^{-3}$ T rms$) \pm 15\%$, $I_r = (30$ A rms$) \pm 25\%$ and $\sin^2 \delta = 0.5$, the force is calculated to be $(3.0 \times 10^{-3}$ N$) \pm 30\%$, in good agreement with the average force measured by the electronic balance, $(3.79 \pm 0.03) \times 10^{-3}$ N.
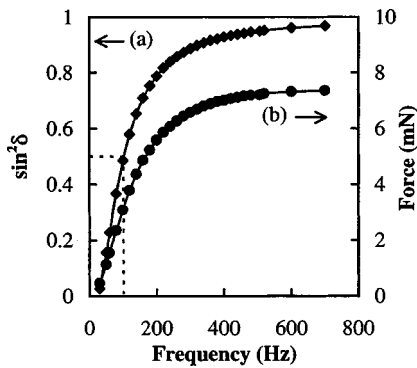
Fig. 3. (a) Measured $\sin^2 \delta$ and (b) time-averaged floating force $\langle F \rangle$ vs frequency, where δ is the phase lag of the ring current I_r. The asymptotic behavior at high frequency is in accordance with Eqs. (5)–(7). The frequency at which $\delta = 45°$ and the force reaches half of its asymptotic value is the corner frequency $f_c = 120$ Hz defined in Eq. (8b).

Fig. 5. Theoretical plot of $\sin^2 \delta$ vs $R/\omega L$ (or f_c/f) taken from Eq. (7). The inductance- and resistance-dominated regimes are shown, along with the three rings which are discussed in this paper: (a) the ring used by Hall,[18] (b) the standard ring supplied with the apparatus, and (c) the custom ring used for the floating measurements.

At a fixed frequency of 120 Hz, we increased the solenoid current above 1 A rms, more than would be sufficient to lift the custom ring off the upright apparatus. The force is proportional to I_{s0}^2 as predicted by Eq. (5) and reported by Hall[18] for a considerably larger ring at higher currents. This result confirms that saturation of the CENCO core is negligible under typical operating conditions, and that its permeability μ is essentially constant, justifying the simple linear inductor model.

In order to compare the results of our custom ring, the larger ring supplied with our apparatus and the ring in Hall's apparatus, we plot $\sin^2 \delta$ vs $R/\omega L$ (or f_c/f), [Eq. (7)] in Fig. 5. The corner frequencies of the three rings (120, 55, and 13 Hz,[18] respectively) have been superimposed on the curve. Figure 5 is divided into regions where the impedance of the ring is dominated either by its inductance ($R/\omega L < 1$) or by its resistance ($R/\omega L > 1$). The large, highly conducting ring used by Hall operates at $f = 4.6 f_c$ at the 60-Hz power line frequency, well into the inductance-dominated region. Our custom ring lies slightly in the resistance-dominated region, and the large ring supplied with our apparatus is almost exactly in the middle. This analysis is important for understanding the behavior of the ring when its resistance is reduced by chilling it in liquid nitrogen (see Sec. V A).

C. Force vs height

Measurements of force versus frequency for various heights of our ring above the solenoid end cap were made to ascertain how the corner frequency and force change as the ring moves away from the solenoid (see Fig. 6). The corner frequency rises slowly from 115 Hz (ring nearly touching the solenoid end cap), to 145 Hz (ring about halfway up the core), then reaches 450 Hz with the ring just above the end of the core. Since the resistance of the ring is approximately $R_r = 4.7 \times 10^{-4} \, \Omega$,[22] the inductance of the ring while resting on the end cap is $L_r = 6.5 \times 10^{-7}$ H in the presence of the core. The rapid increase in f_c occurs as the inductance of the ring falls toward its calculated[23] free-space value of $L_r = 8 \times 10^{-8}$ H.

D. The jumping ring effect

As noted in Sec. I, the naive explanation of the jumping ring (''solenoid magnet repels the induced ring magnet'') is accurate—but only when the electrical transient causes the ring to leave the solenoid in the first quarter cycle of the solenoid current.[11,12] The voltage-controlled jumping ring
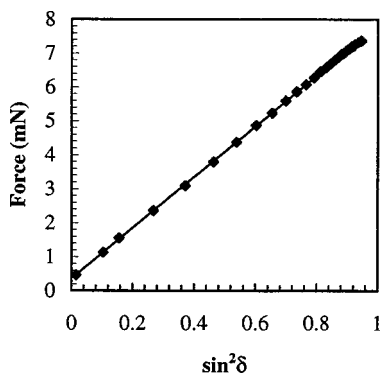

Fig. 4. The time-averaged force $\langle F \rangle$ vs $\sin^2 \delta$ over a frequency range of 20–900 Hz shows the linear dependence expected from the inductive phase lag theory.
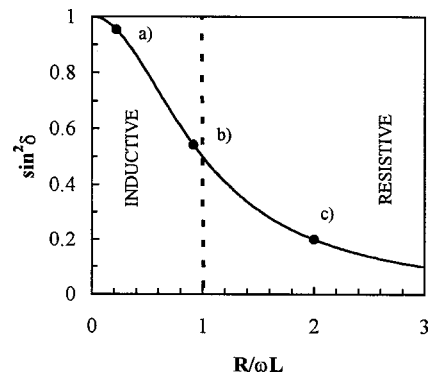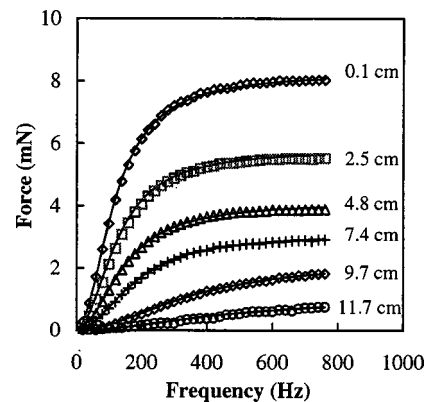

Fig. 6. $\langle F \rangle$ vs frequency at various heights of the ring above the solenoid end cap, along with the fits to Eq. (7), scaled to the high-frequency limit in each case. The corner frequencies increase a factor of 4 (115–450 Hz) over this range in height, while the inductance-limited static force on the ring drops by a factor of 8.
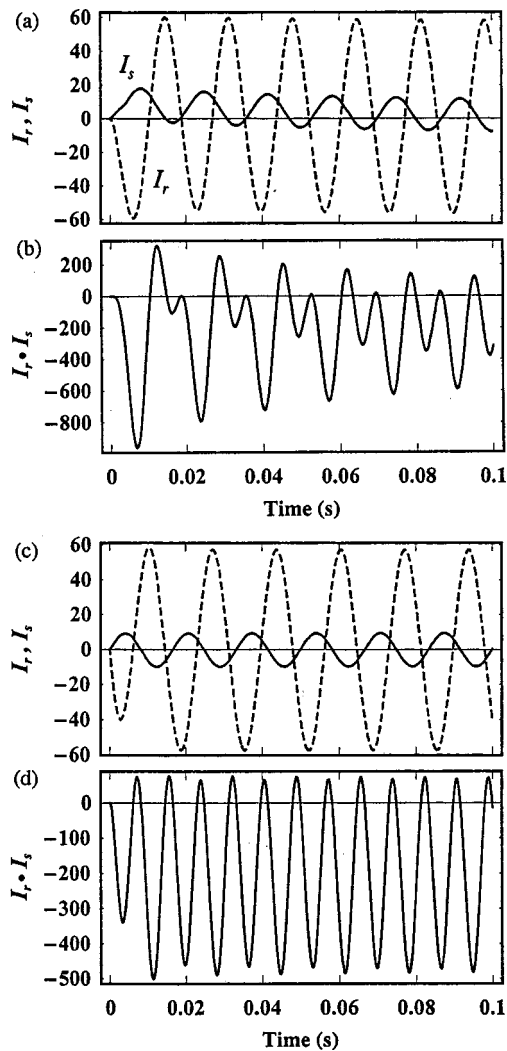
Fig. 7. Simulation of the solenoid current $I_s(t)$ (the smaller value), the ring current $I_r(t)$, and their product $I_s(t) \cdot I_r(t)$, showing the electrical transient when the solenoid is first turned on. Plot (a) shows the largest transients which occur when the line voltage crosses through zero ($\phi=0$) as the current is turned on. Plot (b) shows their product, which can be quite large in the first quarter cycle (negative values of the product indicate a repulsive force). In (c) the line voltage is at its peak ($\phi=\pi/2$) at the moment of turn on. The product of these currents, plotted in (d), shows almost complete absence of the transient and is indistinguishable from the steady state solution.

can be modeled most simply as two inductors (the solenoid and the ring) coupled by a linear mutual inductance:

$$V_0 \sin(\omega t + \phi) - I_s(t)R_s - L_s I_s'(t) - M I_r'(t) = 0$$

$$-I_r(t)R_r - L_r I_r'(t) - M I_s'(t) = 0.$$

Solutions to these equations,[24] $I_r(t)$ and $I_s(t)$, each require a transient of the form $e^{-t/\tau}$, with $\tau = L/R$, in order to satisfy the initial condition $I_r(0) = I_s(0) = 0$. These RL time constants depend upon the respective parameters for the ring and the solenoid. For the CENCO apparatus $R_s = 0.75 \, \Omega$, $L_s = 0.047 \, \mathrm{H}$, so $\tau_s = 0.063$ s, whereas $\tau_r = 1/(2\pi f_c) = 0.003$ s for our large ring at room temperature. The instantaneous force on the ring is proportional to the product of the two currents, $I_s(t) \cdot I_r(t)$, from Eq. (3). Figure 7 plots a simulation of $I_s(t), I_r(t)$, and their product for two different initial

phases $\phi=0$ and $\phi=\pi/2$ of the line voltage, arbitrarily setting $M = 0.03 \cdot (L_s L_r)^{1/2}$ to permit easy comparison of the currents. (The actual ring current is considerably larger than the values shown. By scaling up from our 0.250-A data, we estimate that $I_r = 500$ A rms under these conditions, consistent with a caloric measurement.[25]) Although the additional force due to the transient can initially be quite large (compared to the time-averaged force) when the solenoid is switched on as the line voltage crosses through zero [Fig. 7(b)], the impulse it gives to the ring is a small fraction of the total momentum transferred to the ring, provided the ring stays on the core for many cycles of the power line voltage. If instead the power line voltage is at a peak when the solenoid is turned on, the transient force [Fig. 7(d)] is negligible, and the instantaneous force resembles the steady solution.

Our stroboscopic photographs, taken under conditions that accentuate the effect of the transient ($\phi=0$), show that at modest jump heights (30 cm) the large ring takes six frames (0.1 s) to leave, accelerating until it reaches the height at which it would float. Since the ring stays on the core long after the transient has decayed (given by the shorter time constant $\tau_r = 0.003$ s) the electrical transient accounts for at most a small fraction of the momentum transferred to the ring.

Large, cold rings with lowered resistance should accentuate the effect of the electrical transient by increasing the time constant of the ring; large currents may cause the ring to leave the core over the time scale of the transient, especially for a jumping ring apparatus designed to have a short RL time constant to match that of the ring.[12] Reducing the aluminum ring temperature to 78 K drops its resistance by a factor of 8 or 10 (depending on impurities)[22] and increases the time constant accordingly. Our stroboscopic photographs showed the chilled ring staying on the core for four frames, or 0.07 s, still 2–3 times longer than the time constant of the chilled ring.

Finally, we performed two simple tests to determine whether the transient affects the jump height for rings on our standard apparatus. First, we removed the solid-state relay (which turns on only at the most favorable zero crossing of the input voltage) and measured jump heights by applying 120 VAC of arbitrary initial phase across the solenoid. In a dozen trials the large aluminum ring jumped at 40 ± 1 cm at room temperature, and 88 ± 2 cm at 78 K. This insignificant trial-to-trial variation in jump height indicates that the starting phase of the line voltage is unimportant, and hence that the electrical transient plays no role. Second, we found the same jump height when a room temperature ring was held down and then released, a situation where the transient has long since decayed. The ratio of jump heights for 78 vs 293 K rings (2.2) is readily explained by the time-averaged inductive phase-lag model [Eq. (7)], in that the $f_c = 55$-Hz ring at room temperature has $\sin^2 \delta = 0.54$, whereas the chilled ring with $f_c = 6$ Hz, has $\sin^2 \delta = 0.99$. The ratio of jump heights (assuming that the distance over which the mechanical work is done is the same) is thus predicted to be 1.8. The chilled ring, then, jumps 20% higher than the simple time-averaged inductive phase lag model predicts.

To understand more clearly the increased jump height of the chilled ring, note that the inductance of the solenoid and ring are not constant during the jump (see Fig. 6). As the ring moves up its inductance drops because less of its flux is enhanced by the core; the corner frequency f_c increases. As

f_c exceeds f the force becomes highly dependent on the value of the resistance. Even the largest, best-conducting ring which starts out in the inductance-dominated regime described by Eq. (8c), will enter the resistance-dominated regime in which Eq. (8a) applies, and the increased ring current which flows in the chilled ring can then produce a higher jump.

The chilled jumping ring clearly benefits from the fact that the demonstration is usually done under voltage-controlled conditions. The impedance of the solenoid with the core in place is dominated by its inductive reactance. The presence of the ring on the core causes a back emf arising from the ring current which cancels some of the flux through the solenoid, and hence lowers its impedance. This allows 20% more current I_{so} to flow in the solenoid when the standard ring is resting on the solenoid as compared to when the ring is removed. As the ring jumps, the relatively larger current flowing in the chilled ring causes a further drop in the impedance of the solenoid, raising the current I_{so} and contributing further to the lifting force. Thus we have a two-step mechanism: First, the increase in the corner frequency moves the ring out of the inductance limit, permitting more current to flow in the chilled ring. Then, the greater current in the ring causes the solenoid to draw more current from the power line.

V. SUGGESTED DEMONSTRATIONS

A. The thin chilled ring

The dramatic effect of chilling the ring in liquid nitrogen in order to make it jump high into the air has become a popular extension of the demonstration.[12,15,18] Figure 5 shows that large rings which are already in the inductance-dominated region will not jump much higher with lowered resistance. Conversely, a particularly impressive demonstration using a chilled ring starts with a room-temperature ring in the resistance-dominated regime ($R/\omega L \gg 1$).

By selecting a ring of significantly smaller cross section than the standard ring, and adjusting the solenoid voltage to give an adequate jump at room temperature, one can chill the ring to 78 K and achieve an enormous increase in the height of the jump. A thin copper ring (made from a used ultra high vacuum gasket) which jumps 30 cm at room temperature, jumps over 5-m high after being chilled in liquid nitrogen. A comparison of the ratio of the jump heights (17:1) with the conductance ratio[26,27] for copper (6.7:1) illustrates the significant effect of moving from the resistance (warm ring) to the inductance-dominated (chilled ring) regime.

B. The floating stack of rings

The availability of large numbers of identical thin rings makes possible another intriguing variation on the standard demonstration which does not involve chilling the ring. With the core extended to 10–14 cm, place a single ring on the apparatus and adjust the current so as to float it about halfway up the core. Then place a second ring atop the first. The first will rise up to meet the second ring; as you let go, both rings will settle to float at a higher position than the first ring alone. A third ring will make the stack float still higher. People observing the demonstration may be surprised that despite its growing weight, the stack of rings rises. This effect can be explained by referring to Fig. 5. Consider a single ring of ratio $R/\omega L = 3$ and ignore the (slight) change in in-
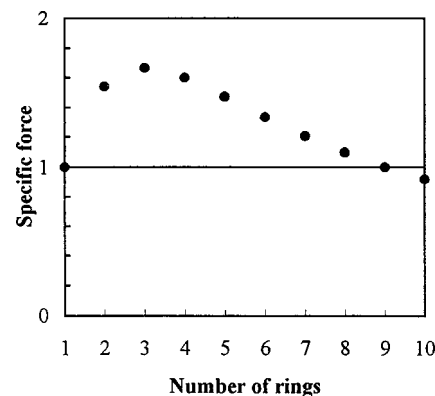

Fig. 8. The specific force (force/weight) vs the number of identical rings for which $R/\omega L = 3$, showing that a stack of such rings will rise until $n = 3$, then fall to the starting height when $n = 9$. Additional rings cause the stack to sink.

ductance (both mutual- and self-) as a second ring is added. We can afford to ignore these changes in M and L since we found that replacing the 6.4 mm high ring in our apparatus with a 12.8 mm ring made from the same tubing stock moves the corner frequency from 120 to 60 Hz, attributable to halving R while keeping L constant. In Fig. 5, then, the second ring moves the stack to $R/\omega L = 1.5$ where the lifting force exceeds the added weight of the ring, so the stack rises.

In general, the force on a single ring is proportional to [from Eq. (7)]

$$F_1 \propto \frac{1}{\left(\dfrac{R}{\omega L}\right)^2 + 1}.$$

This force just balances the weight W of the ring at some initial height above the end cap of the solenoid, so $W = F_1$. The nth ring reduces the resistance of the stack to R/n, so the force on the stack is now:

$$F_n \propto \frac{1}{\left(\dfrac{R}{n\omega L}\right)^2 + 1}.$$

The specific force is the total force divided by the total weight:

$$\frac{F_n}{nW} = \frac{F_n}{nF_1} = \frac{\left(\dfrac{R}{\omega L}\right)^2 + 1}{n\left[\left(\dfrac{R}{n\omega L}\right)^2 + 1\right]}. \tag{9}$$

Solving Eq. (9) for $F_n/nW = 1.0$ (i.e., for when the force on the stack supports the weight of the stack at the initial height of the single ring) yields

$$[n-1]\left[n - \left(\frac{R}{\omega L}\right)^2\right] = 0, \tag{10}$$

which has the trivial solution $n = 1$ (the first ring, by definition, has a specific force of 1), as well as $n = (R/\omega L)^2$. Returning to the example of the single ring for which $R/\omega L = 3$, the specific force is just enough to float the $n = 9$ ring at the starting height. A plot of specific force vs the number of rings for $R/\omega L = 3$ is shown in Fig. 8. The specific force

reaches a maximum when $n = (R/\omega L)$, so the stack should float highest with three rings. This maximum occurs when the corner frequency of the stack equals the driving frequency of the solenoid current. Equation (10) shows that one must begin with $R/\omega L > 2^{1/2}$ in order for a stack of two identical rings to float higher than the height of the first ring, so thin (somewhat resistive) rings are required to demonstrate this effect of the rising stack.

We found that the center of mass of a stack of four of our custom ($f_c = 125$ Hz at a height of 2.5 cm) rings floats at the same height as a single ring when the solenoid is operated at 60 Hz. The second ring causes the stack to rise to its highest point (4.5 cm) and the fifth ring causes the stack to sink to 2.1 cm. To do this experiment carefully, we kept the current in the solenoid constant; otherwise under voltage-controlled conditions it rises approximately 60 mA per ring above the single-ring current of 1.86 A rms. Noting from Eq. (8b) that $R/\omega L = f_c/f = 125$ Hz/60 Hz, Eq. (10) yields $n = (2.1)^2 = 4.3$, in agreement with the experiment.

VI. CONCLUSIONS

Measuring the amplitudes and phases of the magnetic field and ring current in a standard CENCO Thomson's jumping ring apparatus over the frequency range of 20–900 Hz ($0.17f_c$ to $7.5f_c$, where $f_c \equiv R_r/2\pi L_r$), we have found that the static levitating force and jumping height are well explained by the time-averaged force arising from the inductive phase lag of the ring current. The solenoid and ferromagnetic core behave linearly; hysteresis and eddy currents in the core play a minor role, though favorable eddy currents in the retaining clip surrounding the core of the CENCO solenoid contribute an additional short-range lifting force. We found no evidence that the electrical transient affects the jump height either at room temperature or for rings chilled to 78 K. At 60 Hz the impedance of the large standard aluminum ring is dominated by its inductive reactance near the surface of the solenoid, but it can shift into the resistance-dominated regime if the jump is of sufficient height to take the ring above the end of the solenoid. The modestly increased jump height upon chilling the large ring to 78 K is explained by this transition from inductance to resistance dominance, as well as by the observation that the demonstration is performed under constant voltage conditions. The most spectacular effect upon chilling occurs for thin rings which start out in the resistance-dominated regime. We introduce a new variation on the classic floating ring effect wherein a stack of thin rings, despite their greater weight, can float higher than a single ring.

ACKNOWLEDGMENTS

[1] E. Thomson, ''Novel Phenomena of Alternating Currents,'' *The Electrician* (London, June 10, 1887), n.p.

[2] D. O. Woodbury, *Elihu Thomson, Beloved Scientist* (Museum of Science, Boston, MA, 1960, also McGraw–Hill, New York, 1944), pp. 178–180.

[3] J. Abrahams and M. B. Savin, eds., *Selections from the Scientific Correspondence of Elihu Thomson* (MIT, Cambridge, MA, 1971), pp. 233–236.

[4] D. J. Sumner and A. K. Thakkrar, ''Experiments with a 'jumping ring' apparatus,'' Phys. Ed. **7** (4), 238–242 (1972).

[5] B. S. Perkalskis and J. R. Freeman, ''Extending Elihu Thomson's demonstration and Lenz's law,'' Am. J. Phys. **65** (10), 1022–1024 (1997).

[6] H. Fujita, T. Maeda, M. Sakui, F. Nakamura, and H. Inokuchi, ''Calculation method of starting characteristics of single phase linear actuator with open magnetic circuit,'' Trans. Inst. Electr. Eng. Jpn., Part D **116** (9), 963–969 (1996).

[7] P. J. F. Bamji, ''Unconventional electrical machine for circulating molten metal,'' IEE J. Elec. Power Applications **1** (2), 45–53 (1978).

[8] G. Hainsworth, P. J. Leonard, D. Roger, and C. Leyden, ''Finite element modeling of magnetic compression using coupled electromagnetic-structural codes,'' IEEE Trans. Magn. **32** (3), pt. 1, 1050–1053 (1996).

[9] R. P. Feynmann, R. B. Leighton, and M. Sands, *Lectures on Physics* (Addison–Wesley, Reading, MA, 1964), Vol. II, p. 16–5.

[10] D. J. Griffiths, *Introduction to Electrodynamics* (Prentice–Hall, Upper Saddle River, NJ, 1999), 3rd ed., pp. 304–305.

[11] E. J. Churchill and J. D. Noble, ''A Demonstration of Lenz' Law?'' Am. J. Phys. **39**, 285–287 (1971).

[12] C. S. Schneider and J. P. Ertel, ''A classroom jumping ring,'' Am. J. Phys. **66** (8), 686–692 (1998).

[13] G. Carey Foster and A. W. Porter, *Elementary Treatise on Electricity and Magnetism* (Longmans, Green, London, 1903), 2nd ed., pp. 398–399.

[14] L. Page and N. I. Adams, *Principles of Electricity* (Van Nostrand, Princeton, NJ, 1958), 3rd ed., pp. 314–329.

[15] W. M. Saslow, ''Electromechanical implications of Faraday's law: A problem collection,'' Am. J. Phys. **55** (11), 986–993 (1987).

[16] N. Thompson, *Thinking Like a Physicist: Physics Problems for Undergraduates* (Adam Hilger, Bristol, 1987), pp. 24, 106–107.

[17] Y. Mak and K. Young, ''Floating metal ring in an alternating magnetic field,'' Am. J. Phys. **54** (9), 808–811 (1986).

[18] J. Hall, ''Forces on the Jumping Ring,'' Phys. Teach. **35**, 80–83 (1997).

[19] Induction coil, Elihu Thompson type, *Central Scientific Company Catalog J-136* (Central Scientific Company, Chicago, 1936), p. 1300. Our apparatus was obtained in 1936 from this catalog [Grant O. Gale (private communication)].

[20] B. D. Cullity, *Introduction to Magnetic Materials* (Addison–Wesley, Reading, MA, 1972), pp. 49–65.

[21] For a picture of the CENCO apparatus in operation, see the front cover of Ref. 18.

[22] J. R. Davis, ed., *Aluminum and Aluminum Alloys* (American Society for Metals, Metals Park, OH, 1993), pp. 641 and 686.

[23] G. P. Harnwell, *Principles of Electricity and Magnetism* (McGraw–Hill, New York, 1949), 2nd ed., p. 330.

[24] MATHEMATICA 3.0 from Wolfram Research, Inc.

[25] K. E. Jesse, ''Measuring current in a jumping ring,'' Phys. Teach. **35** (4), 198–199 (1997).

[26] G. T. Dyos and T. Farrell, eds., *Electrical Resistivity Handbook* (Peregrinus, London, 1992), p. 207.

[27] *Handbook of Chemistry and Physics* (CRC Press, Boca Raton, FL, 1985), 66th Ed., p. F-120.